Development of a Methodological Approach to Measure Impacts of Reinforcing Steel Corrosion on the Structural Performance of Mid-Rise Concrete Structures During Seismic Events: Its application to Cagayan de Oro City Museum, Philippines

Jose Lorenzo D. Bucton[1*] and Joel G. Opon[2,3]
[1]College of Engineering
[2]Center for Structural Engineering and Informatics
[3]Department of Civil Engineering
Mindanao State University – Iligan Institute of Technology
Iligan City, 9200 Philippines
[*]*joselorenzo.bucton@g.msuiit.edu.ph*

Date received: August 10, 2024
Revision accepted: December 4, 2024

Abstract

The devastating impact of earthquakes on aging reinforced concrete structures is often exacerbated by steel reinforcement corrosion, which significantly compromises their structural integrity. Despite this, many local structural codes lack provisions to address the combined vulnerabilities posed by seismic events and environmental degradation in aging infrastructure. Thus, this study proposes a methodology to quantify the effects of steel reinforcement corrosion on the seismic performance of mid-rise concrete buildings. The approach integrates Fick's second law of diffusion to model time-dependent corrosion and seismic fragility analysis to evaluate structural performance under varying ground motion scenarios. The methodology was validated using the Cagayan de Oro City Museum in Mindanao, Philippines. Results reveal substantial steel area loss due to corrosion, particularly in smaller-diameter reinforcements, leading to weakened structural performance. Fragility curves further demonstrate an increased probability of damage at higher ground acceleration levels, underscoring the critical role of corrosion in amplifying the vulnerability of aging buildings in seismically active regions. These findings highlight the urgent need for enhanced structural assessment frameworks that account for both corrosion-induced deterioration and seismic resilience.

Keywords*:* corrosion, Fick's second law of diffusion, fragility curves, structural integrity, structural performance

1. Introduction

The functionality and strength of structures are critical for ensuring the safety of building occupants during earthquakes. However, many buildings remain highly vulnerable to seismic events or even risk collapse due to structural deterioration, lack of code compliance, and outdated design provisions. Over time, exposure to environmental factors accelerates the decay of building materials (United Nations Environment Programme, 2019). For instance, the degradation of reinforced concrete structures caused by chloride-induced corrosion of reinforcing steel has become a leading factor in infrastructure deterioration worldwide (Mammoliti *et al*., 1996). A notable example is the 2017 Bohol earthquake, which caused significant damage to ten iconic churches in Bohol and Cebu. Among these, the Church of San Pedro Apostol in Loboc—renowned as the second oldest church in Bohol—suffered extensive damage to its main structure, three-story convent, and bell tower (National Museum of the Philippines, 2021).

The structural and economic damages caused by earthquakes on aging structures should not be overlooked, as they pose significant risks to life and property. This is especially crucial in regions frequently affected by destructive earthquakes. The Philippines, located in the Pacific Ring of Fire, is particularly vulnerable to natural disasters, including tropical storms and earthquakes. Earthquakes have gained increasing importance in structural analysis due to the seismic forces they impose. On average, the Philippines experiences three to five mild and harmless earthquakes daily, as most seismic activities in the country are subtle (Silent Gardens, 2017). However, it has also faced major earthquake events, such as the magnitude 6.7 Surigao del Norte Earthquake on February 10, 2017, and the magnitude 7.7 Luzon Earthquake in 1990. Since earthquakes are inherently random events, their occurrence and characteristics are recorded through instrumentation in the form of time-history records.

The combined effects of earthquakes and age-related deterioration, such as steel reinforcement corrosion, are rarely acknowledged. Furthermore, defining the impact of steel reinforcement corrosion on the behavior of aging structures is challenging due to the complexity of the assessment process (Rincon *et al*., 2024). There is a pressing need to understand how age-related deterioration affects the seismic performance of aging and end-of-life structures, as well as to examine the influence of environment-induced corrosion on their behavior. However, local structural codes often lack provisions to address the specific

vulnerabilities of aging structures to seismic events and environmental corrosion. In response, this study aims to develop a methodological approach to quantify the effects of reinforcing steel corrosion on the structural performance of concrete structures during seismic events.

The proposed methodological approach utilizes existing models to probabilistically assess the impact of deterioration through fragility curves. For instance, Fick's second law of diffusion is employed to predict chloride-induced corrosion in concrete reinforcement (Crank, 1975), aiming to define the effective steel reinforcement while accounting for the effects of corrosion over time. Additionally, the Markov chain model, widely recognized for its effectiveness in forecasting the performance of deteriorating structures, is applied to predict cumulative damage in various engineering structures, such as bridges and other infrastructure (Frangopol *et al*., 2015). Fragility curves, on the other hand, serve as essential tools for predicting the extent of probable damage by linking structural damage probabilities to strong motion parameters, thus enabling the estimation of damage likelihood for specific ground motion indices (Karim and Yamazaki *et al*., 2003).

The adequacy of the proposed methodological approach is verified by applying it to assess the fragility of a historical structure—the Cagayan de Oro Museum in Mindanao, Philippines. Colloquially known as the Cagayan de Oro Water Tower, this cylindrical reinforced concrete structure is the city's oldest public building. Constructed between 1921 and 1922, it originally served as a reservoir for water sourced from Malasag Hills. Today, it has been repurposed as the city's museum, bearing witness to a century of local history and evolution. However, due to its age, the structure shows visible signs of wear and tear, raising concerns about its capacity to withstand seismic events. These concerns are heightened by the museum’s location near several active fault lines in the Philippines. In Cagayan de Oro City, three fault lines have been identified: the Central Mindanao Fault (approximately 111.9 kilometers away), the Cabanglasan Fault (134.5 kilometers away), and the newly discovered Tagoloan River Fault, which is the closest at just 22.9 kilometers away.

2. Methodology

2.1 Modelling of Corrosion in Steel Reinforcement

The modeling process for steel reinforcement corrosion, as depicted in Figure 1, aims to calculate the net diameter of the rebar after accounting for the effects of corrosion caused by chloride diffusion. The modeling starts with the calculation of $D(t)$, the diffusion coefficient for chloride ions at age t, following Equations 1 and 2 adopted from Park *et al*. (2016). Subsequent calculations involve determining the maximum crack width, $S_{r,max}$; the crack width diffusion coefficient, D_{cr}; the chloride diffusion coefficient in concrete, D_{cc}; and the crack control, w_k, which denotes crack width in micrometers (μm).

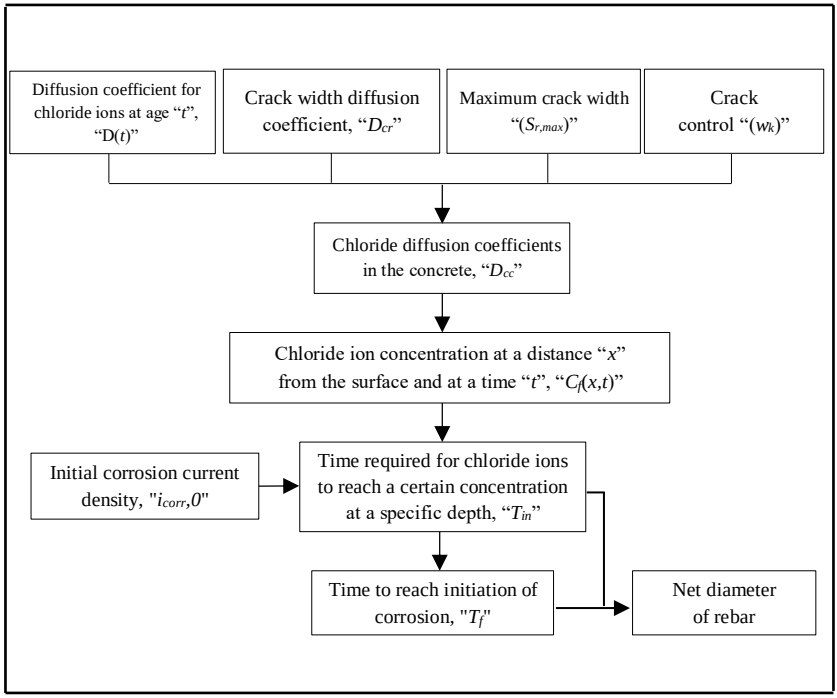

Figure 1. Procedure in modelling of corroded steel reinforcement

Moreover, the previously introduced variables are needed to compute $C_f(x,t)$, the chloride ion concentration at depth x and time t, using Fick's second law. The result is used to determine T_{in} (the time required for chloride ions to reach a certain concentration at a specified depth) and T_f (the time to reach the initiation of steel corrosion). Subsequently, the corrosion density is determined following the method proposed by Vu and Stewart (2000). Finally,

the net diameter of the reinforcing bars is calculated using the approach outlined by Choe *et al*. (2009).

2.2 Time-Dependent Diffusion Coefficient, D(t)

Incorporating time-dependent diffusion coefficients into models enhances the representation of dynamic systems over time. The diffusion coefficient governs particle movement through materials and gradients. Equations 1 and 2 are used to estimate *D(t)*, as adopted from Park *et al*. (2016).

$$m = m_{opc} + \Delta \tag{1}$$

$$D(t) = D_{ref}\left(\frac{t_{ref}}{t}\right)^{m} \tag{2}$$

In Equations 1 and 2, *D(t)* represents the diffusion coefficient at age *t*; D_{ref}, is the reference diffusion coefficient at age t_{ref} (28 days for concrete); *m* is the time-dependent index for chloride ion diffusion; m_{opc} is the diffusion decay coefficient of Ordinary Portland Cement (OPC); and Δ is the increment change of diffusion decay coefficient according to the replacement ratio of admixture, with values from Park *et al*. (2016). The diffusion decay coefficient for chloride ions can be calculated by considering the properties for ordinary Portland cement at 28 days, which in this case, $D_{ref} = 11.64\text{x}10^{-12}\,\frac{m^2}{s}$ and $m = 0.34$ (Park *et al*. 2016).

2.3 Crack Width Control Coefficients, $S_{r,max}$ and w_k

$S_{r,max}$ is defined as the maximum allowable crack width, while w_k pertains to crack control, which is crucial for maintaining structural durability and serviceability. *Eurocode 2* (EN 1992-1-1, 2002) specifies design values for $S_{r,max}$ based on factors such as exposure class, concrete cover, and environmental conditions, expressed in Equation 3. Similarly, the determination of w_k follows the provisions outlined in *Eurocode 2* (EN 1992-1-1, 2002), which aim to limit the width and spacing of cracks in concrete elements. *Eurocode 2* (EN 1992-1-1, 2002) specifies requirements and procedures for managing cracks in structural elements like beams, slabs, and walls. The value of the coefficient w_k is influenced by factors such as concrete characteristics, reinforcement details, and structural loads, as defined in Equation 4 in *Eurocode 2* (EN 1992-1-1, 2002).

$$S_{r,max}=3.4d_c+0.425k_1k_2\frac{d_b}{\rho_{p,eff}} \tag{3}$$

$$w_k=S_{r,max}\frac{\sigma_s-k_{tl}\frac{f_{ctm}}{\rho_{p,eff}}(1+\alpha_e\rho_{p,eff})}{E_s} \tag{4}$$

In Equations 3 and 4, the variables are defined as follows; d_c represents the cover depth; k_1 is the coefficient that accounts for the bond properties of the bonded reinforcement [k_1 is 0.8 for high bond bars and k_1 is 1.6 for bars with an effectively plain surface (EN 1992-1-1, 2002)]; k_2 is the coefficient that accounts the distribution of strain [k_2 is 0.5 for bending and k_2 is 1.0 for pure tension (EN 1992-1-1, 2002)]; d_b denotes the bar diameter; σ_s is the stress in the tension reinforcement, assuming a cracked section; k_{tl} is the factor dependent on the duration of the load [k_{tl} = 0.6 for short term loading and k_t = 0.4 for long-term loading (EN 1992-1-1, 2002)]; α_e is the ratio E_s/E_{cm}; E_s refers to the modulus of elasticity of steel; E_{cm} is the modulus of elasticity of concrete; and f_{ctm} represents the mean value of axial tensile strength of concrete.

2.4 Chloride Diffusion Coefficients, D_{cr} and D_{cc}

The diffusion coefficient through the cracks, D_{cr}, is defined in Equation 5, as adopted from Djerbi *et al*. (2008). The crack width, as previously defined, is expressed in micrometers (μm). Meanwhile, the chloride diffusion coefficient in cracked concrete, D_{cc}, used to estimate the diffusion of chloride ions through cracked concrete elements, can be determined using Equation 6.

$$D_{cr}=\begin{cases}(0.16w_k-3)x\ 10^{-10},\ 30\ \mu m\le w_k\le 100\ \mu m\\ 13\ x\ 10^{-10},\ w_k>\ 100\ \mu m\end{cases} \tag{5}$$

$$\begin{aligned}D_{cc}&=\frac{b\cdot(S_{r,max}-w_k)D(t)+b\cdot w_k D_{cr}}{b\cdot S_{r,max}}\\&=D(t)+\frac{w_k}{S_{r,max}}(D_{cr}-D(t)).\end{aligned} \tag{6}$$

In Equations 5 and 6, *D(t)* represents the diffusion coefficient of chloride ions in sound concrete, and *b* is a parameter that influences the relationship between crack width and the diffusion coefficient. The other parameters are as previously defined. D_{cr} is used to calculate D_{cc}, which also requires the

value of *D(t)*, as shown in Equation 6. The second expression of Equation 6 computes the weighted average of diffusion coefficients, adjusted for crack width relative to $S_{r,max}$. The term $\frac{w_k}{S_{r,max}}$ determines contribution of the crack width diffusion coefficient to the overall chloride diffusion coefficient D_{cc}, while $(D_{cr} - D(t))$ indicates their difference (Djerbi *et al*., 2008).

2.5 Chloride Ion Concentration at Given Time and Depth, $C_f(x,t)$

Estimating the chloride ion concentration profile is essential for evaluating chloride ingress and in assessing the durability of concrete in exposed to chloride-rich environments. The concentration of chloride ions at a specific depth and time within reinforced concrete is calculated using Fick's second law of diffusion, as shown in Equation 7. This law describes the penetration of oxygen into the metal surface, which result in the formation of metal oxides (Gao *et al*., 2017). In Equation 7, $C_f(x,t)$ represents the chloride ion concentration at a distance x from the surface and at a time t; C_f^S denotes the surface chloride concentration; *x* represents the distance from the surface into the concrete; *t* represents the time of exposure to chlorides; and *erf()* represents the error function. For the analysis, the value of *x*, representing the concrete cover, is 40 mm and *t* is 102 years, as detailed in Section 3.1.

$$C_f(x,t) = C_f^S\left[-erf\left(\frac{x}{\sqrt{4 \cdot D_{cc} t}}\right)\right] \tag{7}$$

2.6 Corrosion Initiation Time, T_{in} and T_f

As oxygen reacts with the metal, corrosion initiates and alters the concentration profile. The time required, T_{in}, for chloride ions to reach a specific concentration at a given depth (Gao *et al*., 2017) is calculated using Equation 8. This model predicts variations in corrosion rates over time and under different environmental conditions, such as temperature and humidity. In Equation 8, X_i represents a coefficient associated with the exposure condition and is specific to the chloride ingress model applied; d_c denotes the depth of the concrete where the chloride concentration is evaluated; erf^{-1} refers to the inverse error function; C_{cr} is the critical chloride concentration, defined as the threshold at which reinforcement corrosion may initiate; C_f^s represents the surface chloride concentration; and *n* is a parameter related to the exponent of the chloride diffusion coefficient in the concrete.

$$T_{in}=X_i \frac{d_c^{\,2}}{4D_{cc}}\left[\frac{1}{erf^{1}\left(1-\frac{C_{cr}}{C_f^{s}}\right)}\right]^{n} \tag{8}$$

On the other hand, the time to initiate corrosion, $T_{f,}$ is calculated using Equation 9 as proposed by Gao *et al.* (2017). In Equation 9, d_{bi} represents a coefficient related to the initiation of corrosion, specific to the corrosion model applied; *d* denotes the concrete cover depth, which is the distance between the reinforcement and the concrete surface; and *w/c* represents the water-to-cement ratio.

$$T_f = T_{in} + d_{bi}\left\{\frac{d}{\left[1.0508(1-\frac{w}{c})^{-1.64}\right]}\right\}^{\frac{1}{0.71}} \tag{9}$$

2.7 Net Rebar Diameter Computation, $d_b\,(t|T_{in})$

The net rebar diameter, accounting for the effects of corrosion at time *t*, is expressed in Equation 10. In this equation, $d_b\,(t|T_{in})$ represents the variation of the rebar diameter over time after the initiation of the corrosion process; d_{bo} is the initial diameter of the reinforcement at time $t = 0$; and d_{bi} corresponds to the point at which corrosion-induced cover cracking begins (Gao *et al*., 2017). The remaining variables are as previously defined. Equation 10 accounts for different stages of chloride-induced cover cracking. For times earlier than or equal to T_{in}, the cover cracking remains constant at d_{bo}. For times between T_{in} and T_f, the cover cracking increases based on the difference between d_{bi} and the term $\frac{1.0508\left(1-\frac{w}{c}\right)}{d_c}(t-T_{in})^{0.71}$. After T_f, the cover cracking remains at zero (*0*), indicating that corrosion-induced cracking has initiated.

Additionally, Equation 11 provides an estimate of the initial corrosion current density, $i_{corr,o}$, based on assumptions and models outlined in *Eurocode 2* (EN 1992-1-1, 2002). Whereas, the time-dependent corrosion current density is estimated using Equation 12. This expression follows a power-law relationship, where $(t-T_{in})^{-0.29}$, represents the exponent governing the decay of corrosion current density over time. The factor 0.85 accounts for the reduction in corrosion rate over time (Gao *et al*., 2017).

$$d_b(t|T_{in}) = \begin{cases} d_{bo}, & t \le T_{in} \\ d_{bi} - \dfrac{1.0508\left(1-\dfrac{w}{c}\right)}{d_c}(t-T_{in})^{0.71}, & T_{in} < t \le T_f \\ 0, & t > T_f \end{cases} \quad (10)$$

$$i_{corr,o} = \frac{37.5(1-\frac{w}{c})^{-1.64}}{d_c} \quad (11)$$

$$i_{corr}(t) = 0.85 i_{corr,o}(t-T_{in})^{-0.29} \quad for\ t \ge T_{in} \quad (12)$$

2.8 Development of Fragility Curves

The impact of reinforcement corrosion is assessed through structural analysis using seismic fragility curves, developed via both Nonlinear Static Analysis and Nonlinear Dynamic Analysis, as outlined by Karim and Yamazaki (2001). The process for generating the fragility curves is illustrated in Figure 2. The net steel area, calculated using the method described in the previous section, is used as input alongside the structural model. Structural plans of the target structure are required to develop the model. In this study, the structural modeling is conducted using a building information modeling software (SAP2000 v.21, CSI America, USA). Subsequently, pushover analysis and nonlinear time history analysis are performed. The pushover analysis provides parameter values essential for constructing seismic fragility curves. Additionally, the ground motion data considered for the analysis are presented in Table 1, which was obtained from the PEER Ground Motion Database (PEER, 2023).

The *Section Designer* function in SAP2000 is utilized to create the structural model of the target structure. Key structural properties, such as the building height, are incorporated into the model, along with the application of relevant loads. Pushover hinges are then defined within the model. These plastic hinges represent sections reaching their moment capacity, providing critical data on yield and maximum displacements in SAP2000. The pushover analysis generates a pushover curve, from which the yield displacement and maximum displacement values are derived. These values are essential for calculating ductility factors, which are further validated using results from the time history analysis.

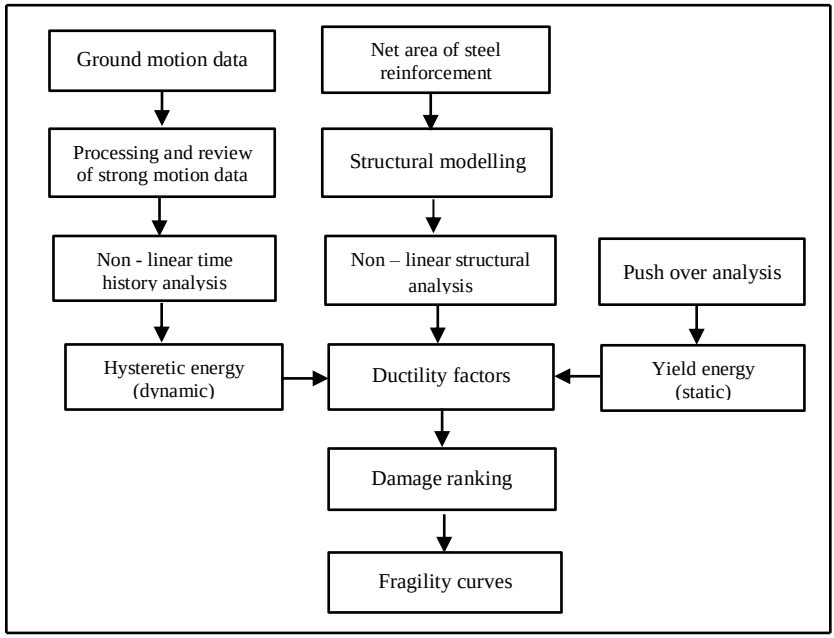

Figure 2. Methodology for Developing Fragility Curves

Table 1. Ground motions utilized for the Non – Linear time history analysis

No.		Station	Magnitude	Year	Fault mechanism
1	Imperial Valley-06a	Coachella Canal #4	6.53	1979	Strike slip
2	Imperial Valley-06b	El Centro array +13	6.53	1979	Strike slip
3	Friuli, Italy-01	Codroipo	6.5	1976	Reverse
4	Parkfield - TM	Temblor Pre 1969	6.19	1966	Strike slip
5	Tabas, Iran	Ferdows	7.35	1978	Reverse
6	Northern California - 01	Ferndale City Hall	6.4	1941	Strike slip
7	San Fernando A	Lake Hughes #12	6.61	1971	Reverse
8	San Fernando B	Lake Hughes #4	6.61	1971	Reverse
9	San Fernando C	Castaic	6.61	1971	Reverse
10	Parkfield - CH	Cholame - Shandon array	6.19	1966	Strike slip

The time history analysis (or nonlinear dynamic analysis) followed the methodology outlined by Karim and Yamazaki (2001). This process involves defining time history functions and ground motion data (see Table 1), with peak ground accelerations (PGAs) ranging from 0.2g to 2.0g, totaling 10 sets of PGAs. After importing the ground motion data into SAP2000 load cases for the nonlinear dynamic analysis were defined. Using the same structural model developed for the pushover analysis, but excluding all pushover load cases, the time history analysis was performed by subjecting the model to each individual ground motion data set. This procedure was repeated for all 10 ground motion data sets. The analysis generated hysteresis models of the structure, which are crucial for determining the maximum displacement of the target structure.

The results of both nonlinear static and nonlinear dynamic analyses are used to calculate the ductility factors defined in Equations 13, 14, and 15. These ductility factors are critical for developing seismic fragility curves (Karim and Yamazaki, 2001). In these equations: μ_u represents the ultimate ductility; μ_d is the displacement ductility; μ_h is the hysteretic energy ductility; $\delta_{max}(static)$ refers to the displacement at maximum reaction from the push over curve (static analysis); $\delta_{max}(dynamic)$ denotes the maximum displacement from the hysteresis model (dynamic analysis); δ_y is the yield displacement from the push-over curve (static analysis); E_h is the hysteretic energy; and E_e represents the yield energy.

$$\boldsymbol{\mu_d = \frac{\delta_{max}(dynamic)}{\delta_y}} \tag{13}$$

$$\boldsymbol{\mu_u = \frac{\delta_{max}(static)}{\delta_y}} \tag{14}$$

$$\boldsymbol{\mu_h = \frac{E_h}{E_e}} \tag{15}$$

After calculating the ductility factors, damage indices can be computed using Equation 16, and are subsequently used to define the damage rank (*DR*). In Equation 16, β is the cyclic loading factor, which is taken as 0.15 for vertical structures. The DRs for each damage index (I_D) are shown in Table 2.

$$I_D = \frac{\mu_d + \beta\mu_h}{\mu_u} \tag{16}$$

Table 2. Damage index (I_D) and State of Structure relationship (adopted from Park and Ang, (1985))

Degree of Damage	Damage Rank	Damage Index (I_D)	State of Structure
No Damage	D	<0.1	Serviceable or localized cracking
Minor Damage	C	0.1 - 0.25	Light cracking throughout
Moderate	B	0.25 - 0.40	Sever cracking, localized spalling
Severe	A	0.40 - 1.0	Severe damage (concrete crushing)
Collapse	As	> 1.0	Loss of building

The damage ratio is defined as the number of occurrences of each damage rank (no damage, minor damage, moderate damage, severe damage, and collapse) divided by the total number of damage states (Park and Ang, 1985). This ratio is plotted against ln (PGA) on a logarithmic scale, from which the mean and standard deviation for the Probability of Exceedance (P_R) curve, defined in Equation 17, can be calculated. The probability of exceedance (P_R) is expressed using Φ, the standard normal distribution function; X, the peak ground acceleration; λ, the mean; and ζ, the standard deviation. By plotting the computed cumulative probability against the peak ground acceleration (PGA), normalized to different excitation, the seismic fragility curve can be derived (see also Karim and Yamazaki, 2001).

$$P_R = \Phi\left(\frac{ln(X) - \lambda}{\xi}\right) \tag{17}$$

2.9 Building Profile of the Cagayan de Oro Museum

The test structure for implementing the method described in the previous sections is the Cagayan de Oro City Museum (Figure 3a), a 102-year-old cylindrical reinforced concrete structure. Originally built as a water tower in 1921-2022, it is the city's oldest structure. The museum's historical significance, coupled with visible signs of structural deterioration, makes it an ideal candidate for testing the proposed method, particularly in assessing its resilience to seismic events. The structural plans for the museum were sourced from the archives of the Bureau of Public Works Quarterly Bulletin (now the Department of Public Works and Highways), Volume 4, No. 3. Based on these

plans, the structure was modeled in SAP2000 (Figure 3b) and subjected to the ground motions detailed in Table 1, forming the foundation for the analysis.

In the SAP2000 environment, the Cagayan de Oro City Museum was symmetrically designed as a cylindrical structure.

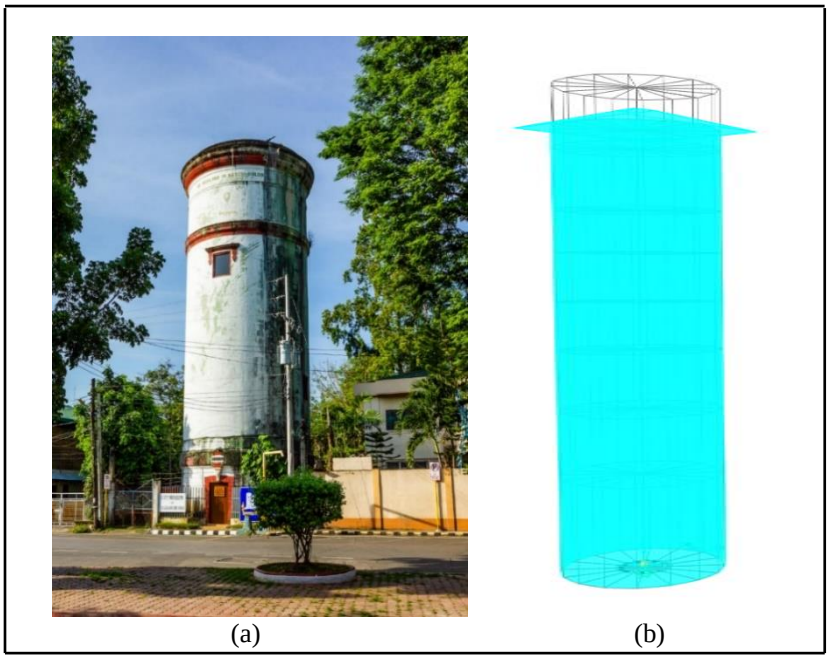

Figure 3. Cagayan de Oro Museum, Philippines: actual photo taken on July 12, 2024 (a) and model in SAP2000 (b)

3. Results and Discussion

3.1 Modelling of Corroded Steel Reinforcement

Modelling corroded steel reinforcement begins with calculating *D(t)*, the diffusion coefficient for chloride ions over time. This involves determining key parameters such as D_a (diffusion coefficient in sound concrete), $S_{r,max}$ (maximum crack width control coefficient), and D_{cr} and D_{cc} (diffusion coefficients related to crack width), using established equations and empirical data. In the analysis the diffusion decay coefficient D_{ref} was assumed to be

$4.99x10^{-12}\frac{m^2}{s}$, considering ordinary Portland cement for a 365-day adapted from Park *et al*. (2016). $S_{r,max}$ and w_k as computed using Equations 3 and 4 and are equal to be 289.9 mm and 0.296 mm, respectively. The secant modulus of elasticity for concrete has a value of 22, 913Mpa (for concrete strength of 21Mpa) from *Eurocode* 2 (EN 1992-1-1, 2002). *D(t)* was computed from Equation 2 to be $1.722354\text{x}10^{-12}\frac{m^2}{s}$, where *t* = 37230 days (age of the structure 102 years) (see also, Park *et al*., 2016).

Following Djerbi *et al*. (2008), since w_k is found to be below 100 μm, D_{cr} is assumed to be $130x10^{-12}\frac{m^2}{s}$, and as for the value of D_{cc}, it is computed to be $3.049810337\text{x}10^{-12}\frac{m^2}{s}$ as per Equation 6. The assumption of the value of D_{cr} is grounded in the empirical findings that w_k influences the rate of crack width diffusion. The values of *D(t)*, D_{cr}, and D_{cc} are used to determine the chloride concentration, $C_f(x,t)$, at a depth of 40 mm (concrete cover). For the current age of the Cagayan de Oro City Museum of 102 years, $C_f(x,t)$ is about $1.271346\frac{kg}{m^3}$ following Equation 7. Moreover, a rebar surface content of free chloride equal to $0.17\frac{kg}{m^3}$ was assumed in this calculation, referring to the work by Gao *et al*. (2017). The value of *Cf(x,t)* could be predicted over time as in Figure 4 and is expected to increase as chloride ions penetrate concrete gradually, driven by environmental factors such as exposure to seawater, deicing salts, or marine atmospheres. This increase directly correlates with the increased risk of chloride-induced corrosion of the reinforcing steel embedded within the concrete (Gao *et al*., 2017). Higher values of $C_f(x,t)$ denote greater chloride exposure and faster corrosion rates.

3.2 Initiation of Steel Reinforcement Corrosion

The theoretical value of the initiation time for steel corrosion is 67.453 years (using Equation 8) and is based on $C_f(x,t)$ ($1.271346\frac{kg}{m^3}$). Specific assumptions were made for this calculation, including a concrete cover depth, d_c of 40 mm for the reinforcing steel as revealed on plans. It is noteworthy that the surface chloride concentration on the concrete varies by location but typically surpasses the critical concentration threshold, C_{cr}. The initiation time signals the start of rebar corrosion and the start of infrastructure deterioration due to corrosion. Similarly, Equation 9 was utilized to estimate the theoretical time when the diameter of the reinforcement reaches zero, resulting in a value of 122.52 years. However, this is of no practical value to the analysis as actual

conditions may vary. The calculation for T_{in} and T_f takes X_i equal to 1 and the water-cement ratio is 0.40, as used in Choe *et al*. (2009).

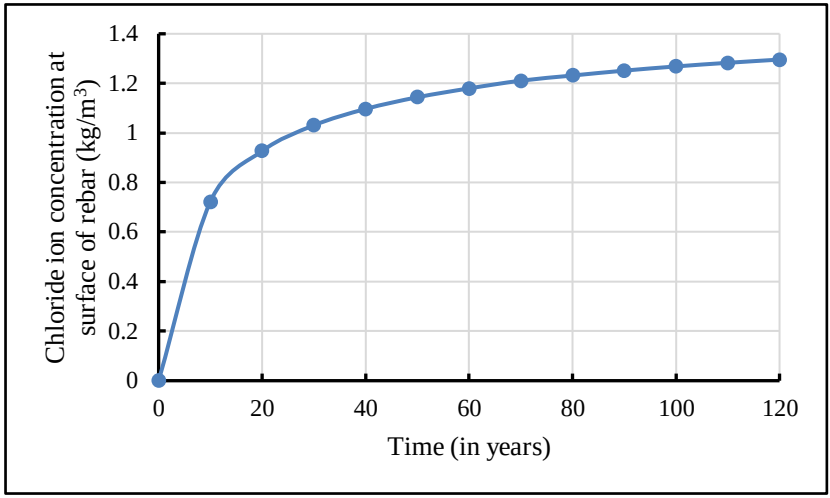

Figure 4. Surface Chloride Ion Concentration on Steel Reinforcement over Time.

3.3 Net Rebar Diameter Computation, $d_b\ (t|T_{in})$

In the investigation of structural integrity over 102 years, Figure 5 provides a visual representation of how the diameter of the primary steel reinforcement (size 25mm) reduces over time due to progressive steel corrosion. The graph demonstrates an average reduction of 2.32 mm in steel reinforcement diameter per decade during the first three decades following corrosion initiation. Beyond this period, the average reduction decreases to 1.63 mm per decade until reaching the T_f.

Based on the current age of the structure, and assuming no intervention has been undertaken, the 25 mm diameter reinforcement is projected to have diminished to approximately 16.37 mm, corresponding to a 56.65% reduction in its cross-sectional area. Furthermore, Figure 6 illustrates the gradual decline in the percentage of the retained reinforcing steel diameter over time. From the figure, it can be observed that less than 40% of the original reinforcing steel diameter remains at the structure's current age of 102 years. This significant loss highlights the critical impact of corrosion on the structural integrity of the reinforcement.

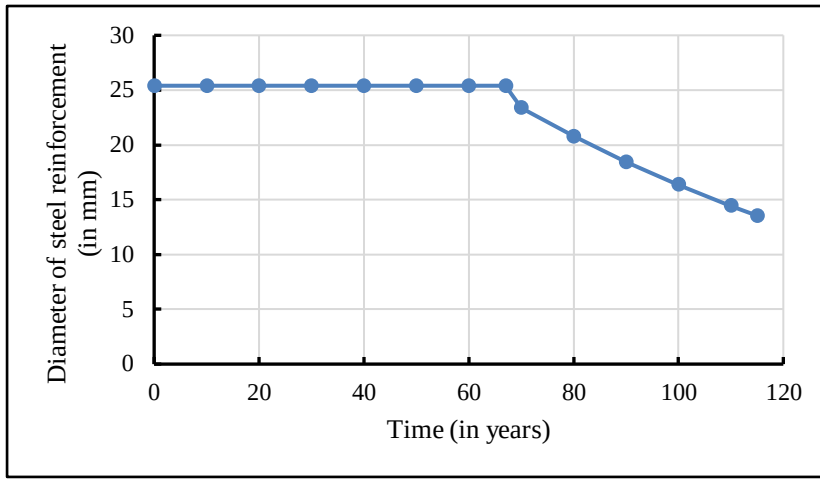

Figure 5. Diameter of Steel Reinforcement (25mm diameter bars) over Time

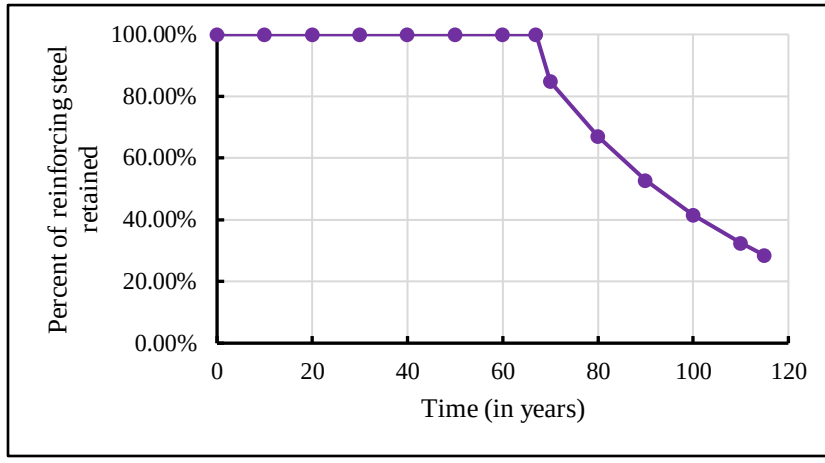

Figure 6. Percentage of Reinforcing Steel retained over Time

3.4 Result of Pushover Analysis and Seismic Fragility Curve

The pushover analysis was performed for both the pristine and corroded conditions, as illustrated by the pushover curves in Figures 7 and 8, respectively. The results reveal significant differences in structural performance between the pristine condition and after 102 years of service. Under pristine conditions (Figure 7), the structure is evaluated to withstand a shear force of approximately 5517.145 kN at a displacement of 0.33696 m. In contrast, after 102 years of service (Figure 8), accounting for deterioration due

to reinforcement corrosion, the museum structure can only sustain a shear force of 2333.784 kN at a displacement of 0.32140 m. This represents a reduction of over 50% in the building's capacity, highlighting the severe impact of rebar corrosion. Similar cases of corrosion-induced degradation have been observed in other structures, such as in Italy (see Granata, 2024), necessitating structural interventions.

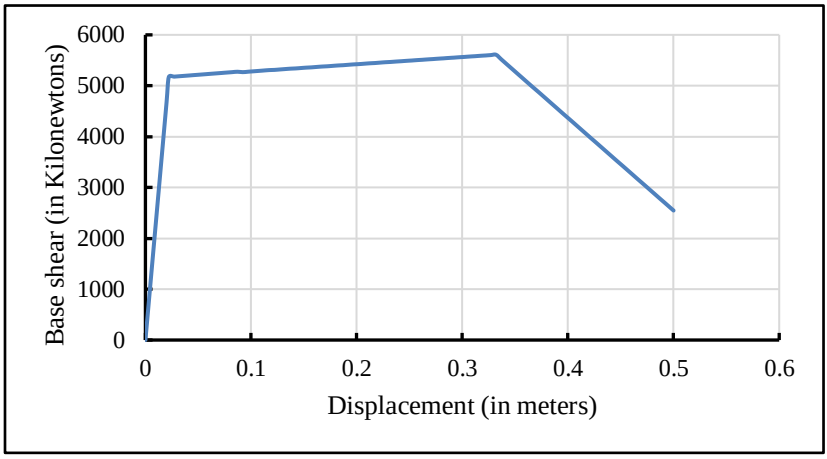

Figure 7. Pushover curve under pristine structural conditions

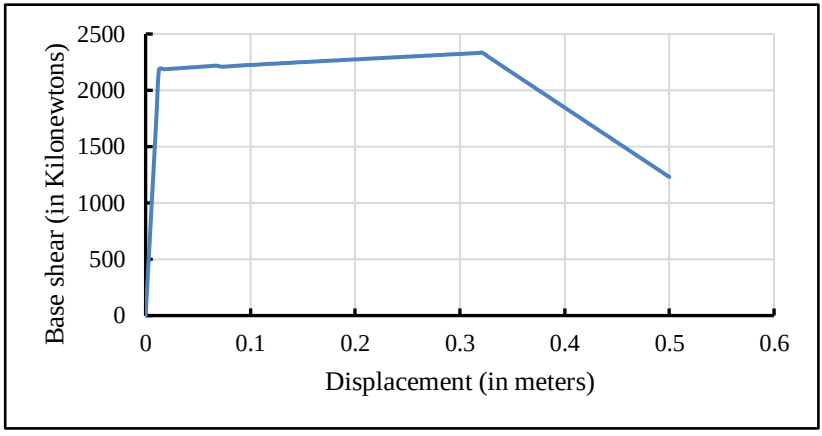

Figure 8. Pushover curve after 102 years of service

Figures 9 and 10 depict the relationship between peak ground acceleration (PGA) and the percentage of structural damage, expressed in terms of damage rank (DR). As PGA increases from 0.2g to 2.0g, the damage states progressively worsen, reflecting increasing severity. This trend is attributed to

the gradual weakening of the structure's strength over time. Under pristine conditions (Figure 9), the structure begins to experience minor damage (damage state C) at higher PGA levels, specifically at 1.8 g and 2.0 g. Conversely, in the corroded condition (Figure 10), higher damage states become prevalent even at lower PGA levels. At higher PGAs (from 1.6 g to 2.0 g), portions of the structure exhibit moderate to severe damage states, underscoring the significant impact of reinforcement corrosion on the structure's seismic vulnerability.

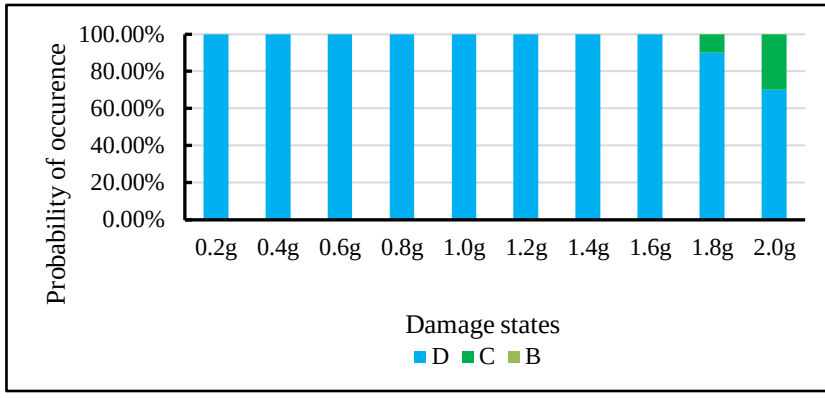

Figure 9. Probability of Occurrence at pristine structural conditions

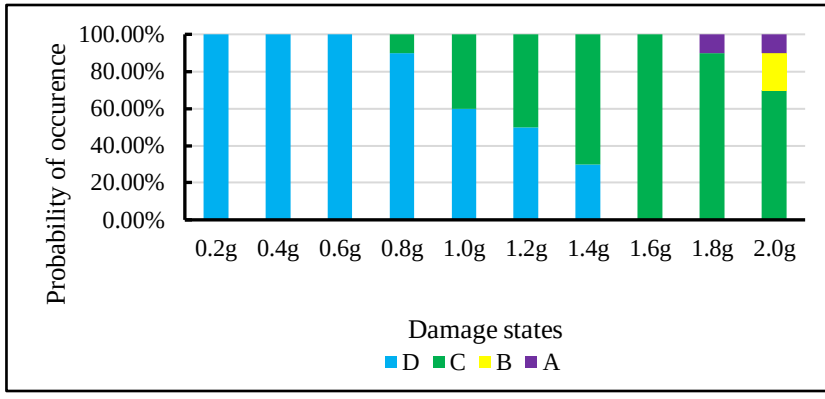

Figure 10. Probability of Occurrence after 102 years of service

The fragility curves for shear failure of the Cagayan de Oro City Museum, under both pristine and corroded conditions, are presented in Figure 11. These curves are overlaid to enable a direct comparison across various damage states. The results underscore that the probability of experiencing higher

damage states increases with peak ground acceleration (PGA) for both conditions. Notably, under the National Structural Code of the Philippines' (NSCP, 2015) design PGA requirement of 0.4g, the fragility curve for the pristine structure indicates a 5.99% probability of slight damage. In contrast, for the corroded 102-year-old structure, this probability rises significantly to 35.02%, highlighting the severe impact of corrosion on the structural vulnerability.

At a PGA of 0.4 g, the pristine structure is not expected to experience moderate or severe damage. However, the corroded condition exhibits distinct vulnerabilities, with a 7.21% probability of moderate damage, a 7.37% probability of severe damage, and a 7.28% probability of structural collapse. These findings highlight the heightened susceptibility of aging structures to severe damage and collapse at higher PGAs. The comparative analysis of fragility curves clearly demonstrates the detrimental impact of steel reinforcement corrosion on the structural capacity of the museum. Similar findings have been reported in other studies. For instance, research on corrosion-affected reinforced concrete structures has shown a significant increase in seismic vulnerability, particularly in structures older than 50 years. Studies by Cui *et al.* (2018) and Pitilakis *et al*. (2014) similarly observed that corrosion-induced degradation significantly increases the probabilities of moderate and severe damage states under seismic loading.

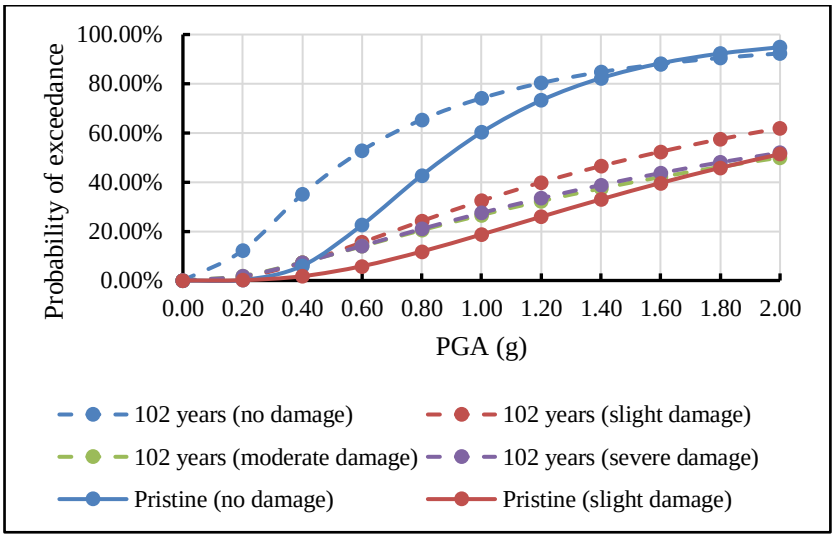

Figure 11. Seismic Fragility curves in both cases

4. Conclusion and Recommendation

This paper proposes a methodology for evaluating the structural performance of mid-rise reinforced concrete buildings, considering the effects of steel reinforcement (rebar) corrosion under varying seismic conditions. The approach incorporates Fick's second law of diffusion to model rebar corrosion, factoring in diverse concrete material conditions, such as the design mix and the presence of cracks. This enables the determination of chloride concentrations at the rebar surface, which is crucial for estimating the initiation time of steel corrosion. Additionally, the method allows for quantifying the reduction in rebar cross-sectional area due to aging. The structural behavior under seismic events, influenced by rebar corrosion, was analyzed using fragility analysis, supported by building information modeling tools and considering multiple earthquake scenarios to perform pushover analysis. The methodology was applied to assess the Cagayan de Oro City Museum in the Philippines – an aging structure exhibiting significant deterioration due to corrosion. Results revealed distinct differences in structural performance between pristine (non-corroded) and corroded conditions. At a peak ground acceleration (PGA) of 0.4g, the pristine structure exhibited a 5.99% probability of slight damage, whereas the corroded structure showed a 35% probability. Moreover, the corroded condition displayed approximately a 7% probability of experiencing higher damage states, with risks increasing at greater PGAs. These findings demonstrate the methodology's efficacy in assessing the effects of corrosion on structural performance and its potential to inform seismic risk mitigation strategies for aging infrastructure. However, the method's technical complexity presents challenges for widespread application. Future research should focus on simplifying the methodology to enhance its accessibility and adoption, enabling practitioners to effectively assess and mitigate risks for deteriorating structures in seismically active regions.

5. Acknowledgement

The authors are grateful to Ar. Aimeelou Jean M. Demetrio, for facilitating access to structural plans; to PEER, for providing ground motion data; to Dr. Michael Bautista Baylon, for guidance in fragility analysis; and to Don G. Bucton, for his unwavering support.

6. References

Association of Structural Engineers of the Philippines (ASEP). (2015). National Structural Code of the Philippines Volume 1: Buildings, Towers, and Other Vertical Structures (7th ed.). ASEP.

Choe, D.E., Gardoni, P., Rosowsky, D., & Haukaas, T. (2009). Seismic fragility estimates for reinforced concrete bridges subject to corrosion. Structural Safety, 31, 275-283. https://doi.org/10.1016/j.strusafe.2008.10.001.

Crank, J. (1975). The Mathematics of Diffusion. Oxford Sci., Oxford, U.K.

Cui, F., Zhang, H., Ghosn, M., & Xu, Y. (2018). Seismic fragility analysis of deteriorating RC bridge substructures subject to marine chloride-induced corrosion. Engineering Structures, 155, 61-72. https://doi.org/10.1016/j.engstruct.2017.10.076

Djerbi, A., Bonnet, S., Khelidj, A., & Baroghel-bouny, V. (2008). Influence of traversing crack on chloride diffusion into concrete. Cement and Concrete Research, 38(6), 877-883. https://doi.org/10.1016/j.cemconres.2007.10.007

EN 1992-1-1 (2002). Eurocode 2: Design of Concrete Structures—Part I: General Rules and Rules for Buildings. European Committee for Standardization.

Frangopol, D., Samantha S., & Mohammed, S. (2015). Maintenance and safety of deteriorating systems: a life-cycle perspective. In D. Fernando, J.G. Ten & J.L. Torero (Eds.), Proceedings of the Second International Conference on Performance-based and Life-cycle Structural Engineering (PLSE2015), Australia, 48-57. https://doi.org/10.14264/uql.2016.1175

Gao, Z., Liang, R.Y., & Patnaik, A.K. (2017). Probabilistic lifetime performance and structural capacity analysis of continuous reinforced concrete slab bridges. International Journal of Advanced Structural Engineering, 9, 231-245.

Granata, M.F. (2024). Seismic retrofit of concrete buildings damaged by corrosion: a case study in Southern Italy. Buildings, 14(4), 1064. https://doi.org/10.3390/buildings14041064

Karim, K.R. & Yamazaki, F. (2001). Effect of Earthquake Ground Motions on Fragility Curves of Highway Bridge Piers Based on Numerical Simulation. Earthquake Engineering and Structural Dynamics, 30(12), 1839-1856. https://doi.org/10.1002/eqe.97

Karim, K. & Yamazaki, F. (2003). A simplified method of constructing fragility curves for highway bridges. Earthquake Engineering & Structural Dynamics. 32. 1603 - 1626. 10.1002/eqe.291.

Mammoliti, L., Brown, L.C.M., & Hope, B. (1996, April). The influence of surface finish of reinforcing steel and pH of the test solution on the chloride threshold concentration for corrosion initiation in synthetic pore solutions. Cement and Concrete Research, 26(4), 545-500. https://doi.org/10.1016/0008-8846(96)00018-X

National Museum of the Philippines. (2021, May 18). Restoration of San Pedro Apostol Parish Church in Loboc completed. Bohol Island News. Retrieved December 13, 2024, from https://boholislandnews.com

Park, J.I., Lee, K.M., Kwon, S.O., & Su-Ho, B. (2016). Diffusion Decay Coefficient for Chloride Ions of Concrete Containing Mineral Admixtures. Advances in Materials Science and Engineering, 5, 1-11. doi: http://dx.doi.org/10.1155/2016/2042918

Park, Y.J. & Ang, A.H. (1985). Mechanistic seismic damage model for reinforced concrete. Journal of Structural Engineering ASCE, 111(4), 740-757.

Pacific Earthquake Engineering Research Center (PEER). (2023). PEER Ground Motion Database. Retrieved from https://ngawest2.berkeley.edu

Pitilakis, K.D., Karapetrou, S.T., & Fotopoulo, S.D. (2014). Consideration of aging and SII effects on seismic vulnerability assessment of RC buildings. Bulletin of Earthquake Engineering 12, 1755-1776. https://doi.org/10.1007/s10518-013-9575-8

Rincon, L.F., Moscoso, Y.M., Hamani, A.E.A, Matos, J.C., & Bastidas-Arteaga, E. (2024). Degradation models and maintenance strategies for reinforced concrete structures in coastal environments under climate change: as review. Buildings, 14(3), 562. https://doi.org/10.3390/buildings14030562

Silent Gardens. (2017). Earthquakes in the Philippines. Retrieved December 13, 2024, from https://www.silent-gardens.com/earthquake-series-2017-were-just-in-time/

United Nations Environment Programme (2019). Report of the United Nations Environment Assembly, 4th Session.

Vu, K.A. & Stewart, M. (2000). Structural reliability of concrete bridges including improved chloride-induced corrosion models. Structural Safety, 22(4), 313-333. https://doi.org/10.1016/S0167-4730(00)00018-7